

## Durham Research Online

---

### Deposited in DRO:

03 January 2012

### Version of attached file:

Submitted Version

### Peer-review status of attached file:

Not peer-reviewed

### Citation for published item:

Damianoglou, Angeliki and Rodger, Alison and Pridmore, Catherine and Dafforn, Timothy R. and Mosely, Jackie A. and Sanderson, John M. and Hicks, Matthew R. (2010) 'The synergistic action of melittin and phospholipase A2 with lipid membranes : development of linear dichroism for membrane-insertion kinetics.', *Protein peptide letters.*, 17 (11). pp. 1351-1362.

### Further information on publisher's website:

<https://doi.org/10.2174/0929866511009011351>

### Publisher's copyright statement:

### Additional information:

PMID: 20673225

---

### Use policy

The full-text may be used and/or reproduced, and given to third parties in any format or medium, without prior permission or charge, for personal research or study, educational, or not-for-profit purposes provided that:

- a full bibliographic reference is made to the original source
- a [link](#) is made to the metadata record in DRO
- the full-text is not changed in any way

The full-text must not be sold in any format or medium without the formal permission of the copyright holders.

Please consult the [full DRO policy](#) for further details.

Copyright © 2010 Pearson Education, Inc. All rights reserved.

Angeliki Damianoglou,<sup>1</sup> Alison Rodger<sup>1</sup>, Catherine Pridmore,<sup>2</sup> Timothy R. Dafforn, Jackie A. Mosely,<sup>2</sup> John M. Sanderson,<sup>2</sup> Matthew R. Hicks<sup>1</sup>

1. Department of Chemistry, University of Warwick, Coventry, CV4 7AL, UK.
2. Department of Chemistry, Centre for Bioactive Chemistry, University Science Laboratories, Durham, DH1 3LE, UK

## Introduction

Membrane proteins make up to 30% of all proteins coded for by most genomes<sup>1</sup> and they facilitate a wide range of cellular functions for the cell and are a means by which the cell communicates with its environment. They are popular drug targets for the pharmaceutical industry.<sup>2</sup> There is also an increasing family of antimicrobial peptides that bind to lipid membranes.<sup>3</sup> The mechanism by which such antimicrobial peptides act has become a complex issue. It is widely accepted that it is important to understand how the peptides act in order to fully exploit the use of peptides as antimicrobial agents.<sup>4</sup> However, the techniques that have been so successfully applied to understand structural questions for globular proteins, including crystallography and NMR, are not as readily applied for the study of membrane proteins. Membrane proteins and peptides are not easy to crystallize and they usually require lipid or detergent environments to remain soluble and folded. Although progress is being made with solution and solid-state NMR the size of the membrane protein-detergent complexes usually results in slow tumbling rates and poor resolution spectra with broad peaks. The other side of the membrane protein-membrane interaction system is the lipid bilayer itself. We currently know very little about how membrane-binding drugs interact with cell membrane lipids. The aim of this work is to explore both sides of this question for the bee venom peptide melittin. By using flow linear dichroism of liposomes a perspective on membrane peptide-membrane interactions becomes available that is not available from any other technique.

Linear dichroism (LD), although not an atomic-level resolution technique, has been found to be ideally suited to membrane environments. Linear dichroism is the differential absorbance of light polarized parallel and perpendicular to an orientation axis. A non-zero signal requires an oriented sample to have absorbance bands in a given region of the spectrum. Following the discovery by Ardhammar et al.<sup>5</sup> that model membranes, known as liposomes, become sufficiently distorted in shear flow to become aligned, together with any molecules bound to the lipid, we showed that membrane peptides and proteins could be flow aligned when

bound to liposomes.<sup>6, 7</sup> As has been illustrated in subsequent work, one can qualitatively and quantitatively identify the orientation of membrane guest molecules, provided that the molecules of interest have significant absorption in the UV-Visible region. One can also measure insertion kinetics in real time to give insight into peptide folding and insertion in membranes.<sup>8-12</sup> In solution, LD has the advantage over other biophysical techniques of being insensitive to off-membrane events—unbound ligands or peptides are invisible as they do not orient.

LD is the ideal technique for probing insertion / binding (or not) into / onto membranes in real time since the signal is zero unless the analyte (for example a peptide) binds to the membrane, and an alpha helical peptide on the surface has opposite signed LD signals to when it is inserted as summarized in Figure .

**Figure Schematic illustration of expected LD signals for an  $\alpha$ -helix on the surface of or inserted in a membrane.**

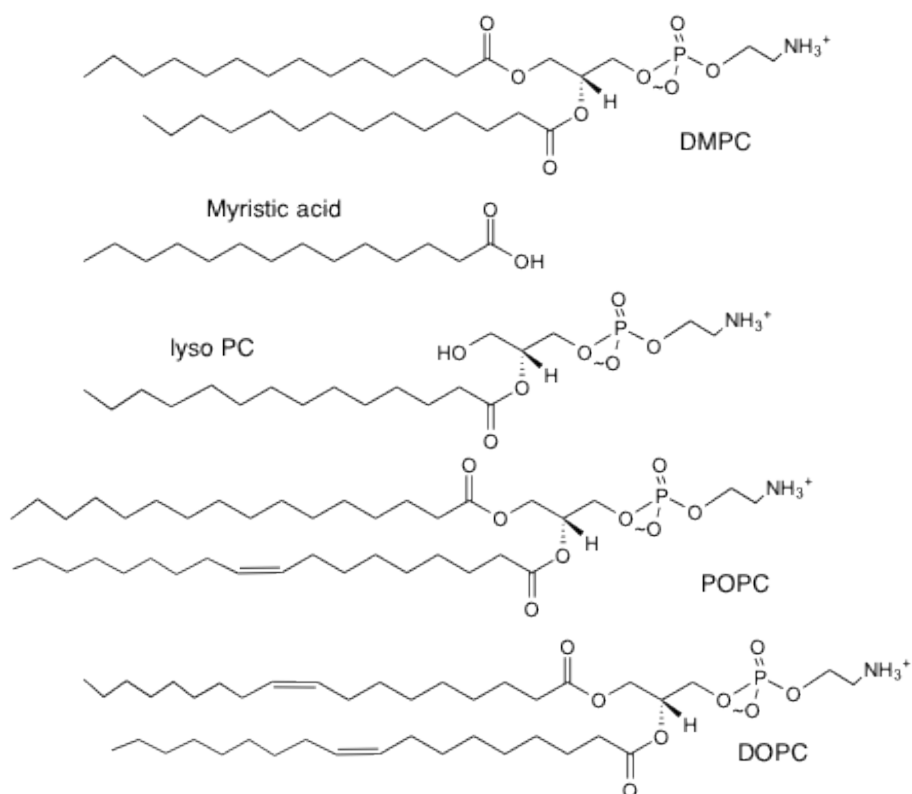
The peptide of interest in this work, melittin, is an amphiphilic and cationic peptide. It is a 26 amino acid residue peptide with a positively charged C-terminus and a proline residue at position 14 that allows it to form kinked helices in non-polar environments.<sup>13</sup> Its secondary structure changes from random coil in aqueous solutions to helical in membranes.<sup>14</sup> At low concentration is in a monomeric conformation, whereas at higher concentrations it forms tetramers in aqueous solution.<sup>14, 15</sup>

Melittin (Figure 2) is an interesting peptide in its own right, being a main component of bee venom and also having anti-microbial properties.<sup>16</sup> In addition it is a popular model peptide for studying cytolytic activities on both eukaryotic and prokaryotic cell membranes. Melittin is known to bind to membranes to form pores, although the mechanism by which it disrupts the membranes is still a matter of debate. Papo and Shai concluded that melittin binds on surface of a membrane or in a transmembrane manner via a carpet-like or barrel-stave mechanism depending on whether it is driven by a combination of hydrophobic or electrostatic effects.<sup>17</sup> Van den Bogaart *et al.* have studied the mechanism of pore formation of melittin in membranes made

from the lipids 1,2-dioleoyl-*sn*-glycero-3-phosphocholine (DOPC) and 1,2-dioleoyl-*sn*-glycero-3-[phospho-*rac*-(1-glycerol)] (DOPG). They concluded that melittin caused pore formation in DOPC membranes but not those made of DOPG.<sup>18</sup> Most recently Manna *et al.* concluded from modeling that in 1-palmitoyl-2-oleoyl-*sn*-glycero-3-phosphocholine (POPC) membranes melittin forms pores in the membrane by the toroidal mechanism.<sup>19</sup> The peptide's behaviour in membranes depends on many variables such as the concentration of the peptide, the composition and phase of the lipid membrane or even the solvents and buffers used to carry out the experiments.

(a) **NH<sub>2</sub>-GIGAVLK<sup>+</sup>VLTTGLPALISWIK<sup>+</sup>R<sup>+</sup>K<sup>+</sup>R<sup>+</sup>QQ-CONH<sub>2</sub>**

(b)



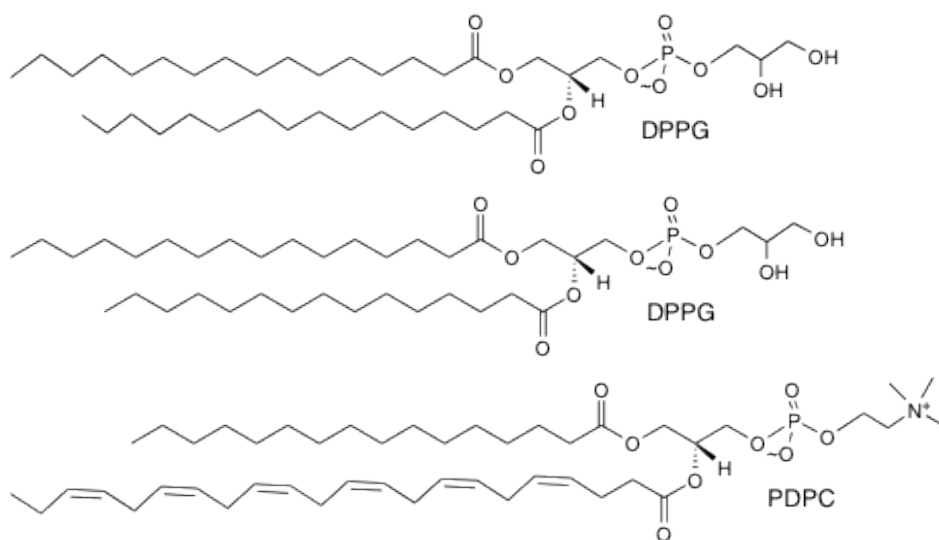


**Figure** (a) Sequence of melittin. (b) Structures of lipids of relevance to this work: DMPC, myristic acid, lyso PC, 1-palmitoyl-2-oleoyl-*sn*-glycero-3-phosphocholine (POPC), 1,2-dioleoyl-*sn*-glycero-3-phosphocholine (DOPC), 1,2-dipalmitoyl-*sn*-glycero-3-phospho-(1'-*rac*-glycerol) (DPPG), 1,2-dipalmitoyl-*sn*-glycero-3-phosphocholine (DPPC).

In bee venom, melittin is always accompanied by the enzyme phospholipase A2 (PA2). Melittin and PA2 are known to act synergistically on cell membranes: melittin enhances the movement of anions in membranes and lyses cells at high concentration, this is facilitated by the lipolytic activity of PA2 which catalyses the hydrolysis of the *sn*-2 ester bond of lipids in the presence of  $\text{Ca}^{2+}$ .<sup>20</sup> Conversely, melittin enhances the rate of hydrolysis by perturbing the lipid bilayer and reorienting the *sn*-2 ester bond. Of particular relevance to this work, PA2 is known to hydrolyse the lipid 1,2-dimyristoyl-*sn*-glycero-3-phosphocholine (DMPC, Figure 1) to form lyso MPC and myristic acid.<sup>21</sup>

In this work we have used LD, complemented by other spectroscopic techniques as well as dynamic light scattering (DLS) and MALDI mass spectrometry, to probe the behaviour of melittin inserting into different membrane-mimicking lipid environments and to consider the effect of the enzyme PA2 on that process. The lipids vary in their acyl chain length, degree of unsaturation and charge. By complementing LD with a range of other biophysical techniques including circular dichroism (CD), MALDI-MS, thin layer chromatography (TLC), DLS and oriented CD (OCD) we have been able to follow the folding and insertion process of melittin into membranes in real time and to understand key aspects of the process. Most of the work has

been undertaken with melittin co-purified with trace amounts of PA2 present ( $<0.05$  U/mg), denoted melittin<sup>PA2</sup>. However control experiments on isolated melittin (melittin<sup>pure</sup>), phospholipase A2, and a controlled mixture of the two have also been undertaken.

## **Materials and methods**

### ***Materials***

Melittin from bee venom was purchased from Sigma-Aldrich (Dorset, UK). This melittin is co-purified with PA2 ( $<0.5$  U/mg). Bis-tris propane (B6755)  $\text{CH}_2[\text{CH}_2\text{NHC}(\text{CH}_2\text{OH})_3]_2$  was purchased from Sigma-Aldrich. Its pH was adjusted with diluted hydrochloric acid. DMPC, 1-palmitoyl-2-oleoyl-*sn*-glycero-3-phosphocholine (POPC), 1,2-dioleoyl-*sn*-glycero-3-phosphocholine (DOPC), 1,2-dipalmitoyl-*sn*-glycero-3-phospho-(1'-*rac*-glycerol) (DPPG), 1,2-dipalmitoyl-*sn*-glycero-3-phosphocholine (DPPC) and 1-palmitoyl-2-docosahexaenoyl-*sn*-glycero-3-phosphocholine (PDPC) were purchased from Avanti polar Lipids, Alabama, USA. All other chemicals were obtained from Sigma-Aldrich.

### ***Methods***

#### ***Liposome preparation***

A stock solution of 2.5 mg/mL small unilamellar vesicles (SUVs) was prepared by dissolving the lipid (or lipids) in either 2,2,2-trifluoroethanol (DMPC) or chloroform (the remainder). The sample was then dried under nitrogen flow and placed under vacuum overnight to remove residual organic solvent resulting in a lipid film on the inner surface of the container. The lipid film was then suspended in 10 mM bis-tris propane (BTP, 10 mM, pH 7) and freeze/thawed five times using dry ice/ethanol and room temperature (RT) for DMPC, DOPC, POPC and PDPC and dry ice/ethanol and 37 °C for DPPC, DPPG, POPC/DPPG. The lipid samples were then extruded 11 times through a 100 nm polycarbonate membrane, at temperatures similar to those used during the thawing process to create nominal 100 nm liposomes (the actual size of the liposomes is larger once they relax following extrusion as discussed below).

#### ***Peptide solutions***

The peptide was dissolved in water to produce stock solutions of 5 mg/ml. Experiments were all undertaken at lipid:peptide molar ratio of 100:1 and peptide concentration of 0.1 mg/mL. Samples were prepared by adding the appropriate volume of the peptide stock solution to a buffered solution of liposomes.

### ***Spectroscopy***

CD spectra were collected in a 0.5 mm path length quartz demountable cell in a Jasco (Great Dunmow, UK) J-815 CD spectropolarimeter. LD spectra were collected using a Jasco J-815 spectropolarimeter adapted for LD measurements in a microvolume Couette flow cell manufactured by Crystal Precision Optics, Rugby, UK and now available via Kromatek Ltd., (Great Dunmow, UK).<sup>7, 10-12, 22-26</sup> Far UV CD and LD spectra (190–320 nm) were collected using a data pitch of 0.2 nm, continuous scanning mode, scanning speed of 100 nm/min, response of 1 s, band width of 1 or 2 nm. The Couette cell rotation speed was ~3000 rpm (setting: 3.0 V). Fluorescence spectra were collected using a Jasco FP-6500 fluorimeter using excitation wavelength 280 nm, with 3 nm bandwidth for excitation and emission, and 3 mm path length microvolume cuvettes (Starna Hainalt, UK). DLS data were collected using a Malvern Zetasizer Nano S (Malvern Instruments, Malvern, UK) and the 3 mm path length microvolume fluorescence cuvette. Samples for OCD were deposited on a flat cylindrical quartz cuvette and allowed to dry overnight before being inserted into the light beam with the light beam incident perpendicular to the plane of the quartz.

### ***MALDI***

Melittin<sup>PA2</sup> was added to DMPC liposomes in 10 mM bis-tris propane (pH 7) in the absence of EDTA, and 1  $\mu$ l aliquots were removed every 30 seconds and immediately mixed with a solution of 2,5-dihydroxybenzoic acid (DHB) matrix (9  $\mu$ l, 10 mg/ml, water/0.1% TFA). The addition to the matrix solution was found, in preliminary previous experiments, to quench the hydrolysis-catalysing effect of the enzyme PA2. Two aliquots of 0.6  $\mu$ l of each sample were spotted on separate positions on the MALDI target plate. MALDI-MS spectra were recorded, using a Ultraflex II MALDI-TOF/TOF spectrometer with 337 nm nitrogen laser (Bruker Daltonics Ltd., Coventry, UK) for each aliquot the intensity of the peak corresponding to lyso-MPC was normalized relative to that of the sum of the peaks corresponding to lyso-MPC and the [DMPC + H]<sup>+</sup> molecular ion. Data were averaged over 4000 laser shots from each spot. The error bars correspond to two times the standard deviation of the data from the two spots.

### ***Results***

We first consider the secondary structure of melittin in a range of lipids. An analysis of data collected during the binding of melittin with DMPC liposomes is then followed by an overview of its behaviour with a range of other lipids. The key properties of the lipids used in this work are summarized in Table . The variables include charge and unsaturation as well as chain length.

**Table Properties of lipids used in this work, the orientation of melittin on or in the liposome, and the ratios of the melittin CD signals at 222 nm and 208 nm. The notation 18:2 denotes a lipid tail length of 18 carbons with 2 unsaturated bonds. DMPC at 25° C is very close to its phase transition temperature (23° C for pure DMPC) as denoted by the phase assignment of “transition”.**

| Lipid          | Lipid charge<br>And phase | Degree of<br>unsaturation | Melittin                       | Orientation<br>on or in<br>membrane | CD <sub>222</sub> /CD <sub>208</sub> | Fluorescence<br>maximum |
|----------------|---------------------------|---------------------------|--------------------------------|-------------------------------------|--------------------------------------|-------------------------|
| DOPC           | +/- (liquid)              | 18:1_18:1                 | Melittin <sup>PA2</sup>        | In                                  | 1.4                                  | 336                     |
| POPC           | +/- (liquid)              | 18:1_16:0                 | Melittin <sup>PA2</sup>        | In                                  | 1.2                                  | 335                     |
| 80POPC:20DPPG  | - (liquid)                | 18:1_16:0/16:0            | Melittin <sup>PA2</sup>        | In                                  | 1.2                                  | 336                     |
| DPPG           | - (gel)                   | 16:0                      | Melittin <sup>PA2</sup>        | In                                  | 0.96                                 | 333                     |
| 80DPPC:20DPPG  | - (gel)                   | 16:0/ 16:0                | Melittin <sup>PA2</sup>        | In                                  | 1.04                                 | 335                     |
| DPPC 37 °C     | +/- (liquid)              | 16:0                      | Melittin <sup>PA2</sup>        | -                                   | 0.92                                 | 339                     |
| DMPC 37 °C     | +/- (liquid)              | 14:0                      | Melittin <sup>PA2</sup>        | In                                  | 1.05                                 | 338                     |
| DMPC 25 °C LUV | +/- (transition)          | 14:0                      | Melittin <sup>PA2</sup>        | In                                  | 1.05                                 | 335                     |
| DMPC 25 °C SUV | +/- (transition)          | 14:0                      | Melittin <sup>PA2</sup>        | In                                  | 0.99                                 | 335                     |
| DMPC 37 °C     | +/- (liquid)              | 14:0                      | Melittin <sup>pure</sup>       | In                                  | 0.87                                 | 341                     |
| DMPC 37 °C     | +/- (liquid)              | 14:0                      | Melittin <sup>pure</sup> + PA2 | In                                  | 0.96                                 | 342                     |

### ***Secondary structure of melittin***

Melittin is known to be unfolded in aqueous solution and to be folded into an  $\alpha$ -helix when in the presence of any lipids for which the CD has been measured.<sup>27, 28 29,30-32</sup> Melittin's CD spectra in water and in lipid (DMPC) are illustrated in Figure a. The secondary structure of melittin in DMPC is established within the dead-time of loading the cuvette and remains unchanged thereafter (Figure b).

In this work, for the first time, the effect of lipid unsaturation and lipid charge on the CD spectra of melittin has been investigated. The concentration of PA2 in all samples was so low that it makes no direct contribution to the CD spectra. As shown in Figure c, the melittin CD spectra are all indicative of it having a helical conformation and they are very similar in magnitude, but vary slightly in shape as a function of lipid composition of the membrane. The intensity of the CD spectra of melittin at 222 nm are larger than those at 208 nm when melittin is inserted (see below for proof of insertion by LD) in membranes made of unsaturated lipids and conversely for saturated lipids, as summarized in Table . The CD<sub>222</sub>/CD<sub>208</sub> ratio is associated in the literature with the hydrophobicity of the environment of a helical peptide (originally methanol versus lipid)<sup>33</sup> as well as its oligomeric state (oligomerisation presumably also providing a more hydrophobic environment). For example, larger CD<sub>222</sub>/CD<sub>208</sub> ratios have been deemed to indicate membrane insertion or oligomerisation.<sup>34, 35</sup> Although this has not been proven, the idea is sufficiently widely used that we can conclude it is consistent with most data that have been collected. Our results therefore imply that the unsaturated lipids provide a more



hydrophobic environment for melittin. In support of this, the fluorescence maximum of melittin's tryptophan shifts to lower wavelength (which also implies a more hydrophobic environment) with increasing lipid unsaturation (Table ). It therefore follows that increasing unsaturation enables the lipids to pack about the helix more effectively. We attribute this effect to membrane flexibility and packing. Consistent with this, melittin with PA2 and melittin with mixed lipids (all where the membrane is more flexible) have higher  $CD_{222}/CD_{208}$  ratios. We return to this issue below.

There is one report in the literature of melittin becoming a  $\beta$ -sheet in a lipid with 6 double bonds, 1-palmitoyl-2-docosahexaenoyl-*sn*-glycero-3-phosphocholine (PDPC). The observed loss of the CD signal at 208 nm that has been attributed to a  $\beta$ -sheet structure,<sup>36</sup> is almost certainly a spectral artifact, as the published spectrum is actually closer to that expected for an  $\alpha$ -helix<sup>24</sup> combined with the artifacts that arise from the saturation of the photomultiplier tube.<sup>37</sup> To confirm this is actually the case we measured the *CD* spectrum of melittin when added to PDPC liposomes and after 20 hours. Both spectra are clearly  $\alpha$ -helical, though with the highest 222 nm/208 nm ratio which supports the above conclusion about hydrophobic environment being provided by unsaturated lipids. Infra red data (not shown) confirm the lack of  $\beta$  structure for melittin with this lipid.

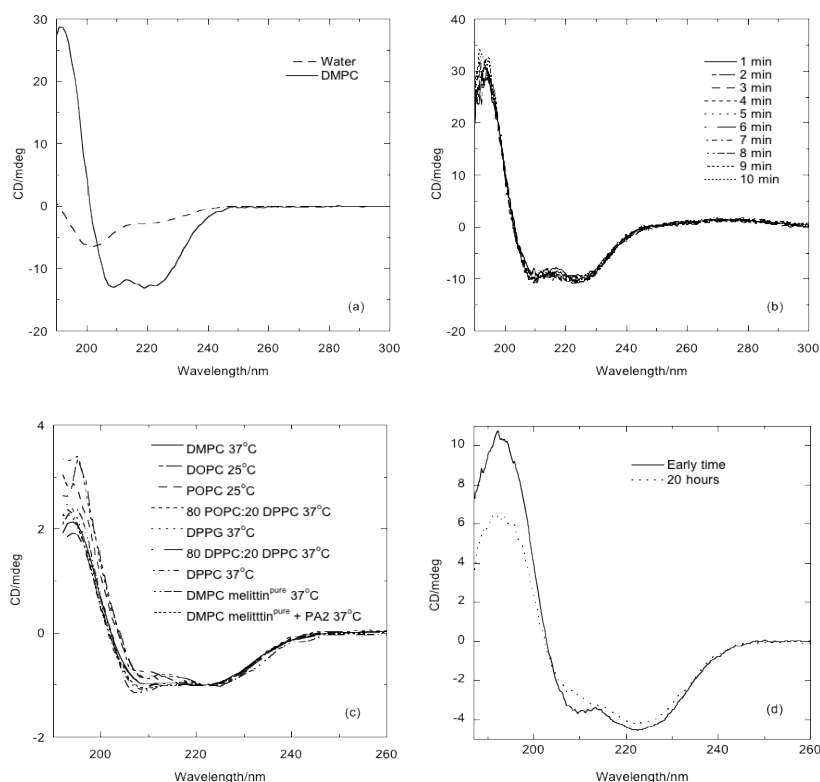


**Figure** CD spectra of melittin (0.1 mg/mL) in 0.5 mm path length cuvettes as a function of lipid environment (lipid:melittin molecular ratio 100:1). (a) Melittin<sup>PA2</sup> in DMPC and water at 25°C. (b) Melittin<sup>PA2</sup> in DMPC at 25°C as a function of time. (c) Melittin in different lipids and temperatures (as indicated in the figure). Melittin is melittin<sup>PA2</sup> unless otherwise indicated. (d) Melittin<sup>pure</sup> in PDPC.

#### *Interaction of melittin<sup>PA2</sup> and melittin<sup>pure</sup> with DMPC*

Our aim, for the first time, was to probe the insertion of melittin into lipid bilayers in aqueous solution in real time. As shown in **Figure**, at time zero (when the melittin is already helical as shown by CD, Figure a) at both 25°C and 37°C, for melittin<sup>PA2</sup> and DMPC liposomes, LD~0. After a few minutes at both temperatures a positive LD signal is apparent in the region of 224 nm and 192 nm. The minimum at 210 nm is in fact the negative signal from the long wavelength component of the  $\pi$ - $\pi^*$  transition (Figure). Since  $\alpha$ -helix transitions at 222 nm and 192 nm are polarized perpendicular to the helix axis and that at 210 nm is polarized parallel to the helix axis,<sup>22</sup> and since for liposome-bound chromophores<sup>5,22</sup>

where  $S$  is the orientation parameter,  $\beta$  is the angle between a transition moment and the normal to the bilayer surface and  $A_{iso}$  is the isotropic absorbance of the sample (i.e. the unaligned sample), it follows that the melittin is inserting into the bilayer after the first few minutes with either its orientation becoming more parallel to the membrane normal as time goes on or more melittin inserting.

Given that the  $\alpha$ -helical CD signature of melittin with DMPC tells us that it is membrane associated (see above) from the beginning of the LD experiment, it is intriguing that the initial LD is zero. If the melittin  $\alpha$ -helix is lying flat on the surface then its LD sign pattern should simply be approximately opposite from that observed at later time as illustrated in Figure . The only other option for having LD=0 is that the dominant 222 nm and 192 nm bands are oriented with transition moments having average orientation close to the magic angle  $\beta=54.7^\circ$ . Since melittin is known to kink at its central proline, the LD therefore suggests that the kink angle is  $\sim 110^\circ$  as illustrated in Figure .

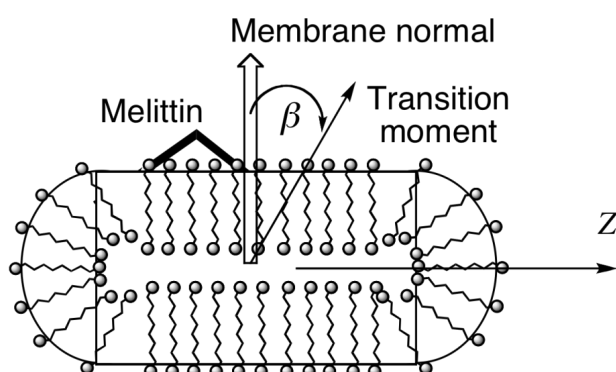


**Figure** Schematic illustration of melittin (bold lines) bound on the surface of the liposome with the backbone lying at the magic angle to the membrane normal.

The insertion kinetics of melittin with DMPC liposomes are much faster at  $25^\circ\text{C}$  than at  $37^\circ\text{C}$  (**Figure** ). Further, by  $t=6$  minutes the  $25^\circ\text{C}$  melittin LD is back to zero, whereas the  $37^\circ\text{C}$  signal begins to decrease only after hours. The reason for the LD at  $25^\circ\text{C}$  having vanished by  $t=6$  minutes is apparent from the DLS data (Figure 6a): the average vesicle size increases from its initial value of about 180 nm to 240 nm at 3 minutes and then dramatically drops to 25–35 nm. These particles are too small or too rigid to orient in the Couette flow. The  $37^\circ\text{C}$  data, by way of contrast, shows a gradual increase in LD and no micellisation. The DMPC liposomes alone

remain the same size over time, measured using DLS (data not shown). The oriented CD spectra of Figure b, measured on a 25°C sample collected at the conclusion of its kinetic process and then dried onto a flat surface, show that the melittin is still inserted into the bilayer in a trans-membrane orientation (the 208 nm band is attenuated compared with the spectra of Figure and the 192 nm band shifts to longer wavelength).<sup>37</sup>

Performing the LD/DLS experiment at other temperatures (21°C, 25°C, 29°C, 35°C and 37°C, data not shown) indicated that at the lower temperatures rapid fusion of liposomes followed by lipid micellisation occurs yet at 35°C and 37°C only gradual fusion of the liposomes occurs. The DMPC phase transition is at 23°C so near the phase transition is where we observe micellisation to occur. It is somewhat counter-intuitive that the insertion is faster in the more rigid lower temperature environment. We return to this below.

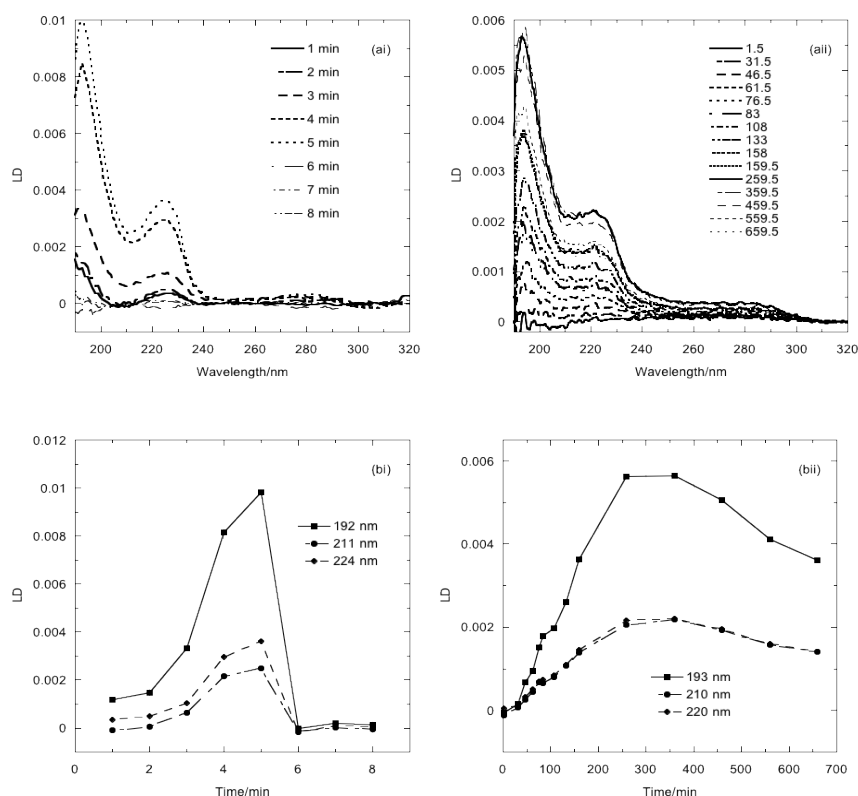


**Figure** LD of melittin<sup>PA2</sup> (0.1 mg/mL) when added to DMPC liposomes (at molar ratio of lipid: peptide of

100:1) at (i) 25 °C and (ii) 37°C. (a) Wavelength scans. (b) Data plotted as a function of time at selected wavelengths.

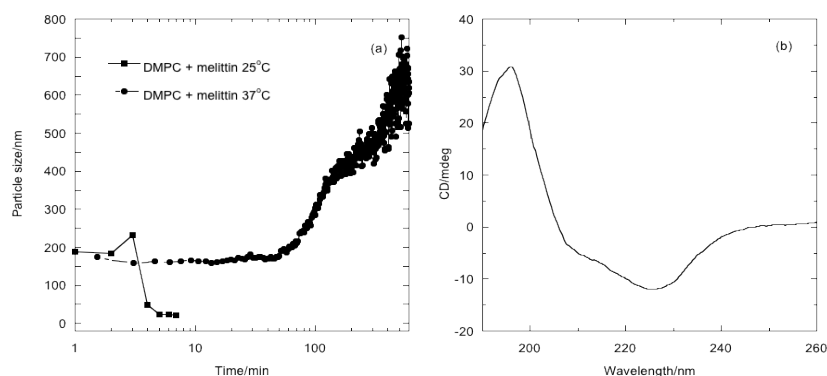


**Figure** (a) DLS of DMPC liposomes after addition of melittin<sup>PA2</sup> (0.1 mg/mL) (at molar ratio of lipid: peptide of 100:1) at 25 °C and 37°C. (Note log scale on x-axis.) (b) OCD of the 25°C sample at the end of the kinetics after the water has been evaporated.

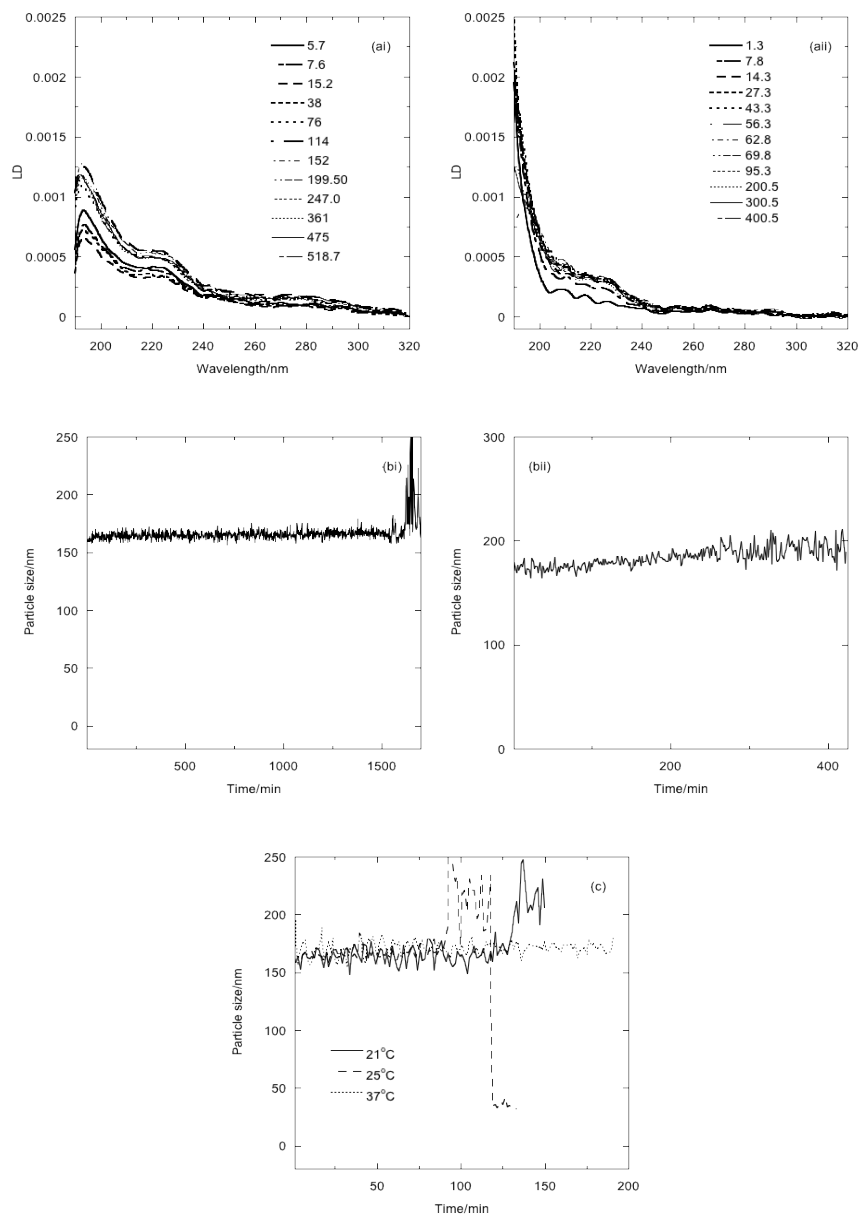
### *The role of PA2 in melittin insertion kinetics*

Since it is known that PA2 hydrolyses lipids and since we see a change (albeit small) in the CD spectrum of melittin with and without catalytic amounts of PA2, we were interested to see how PA2 affected the insertion kinetics of melittin. The data of **Figure** and Figure show that the same kind of insertion and liposome growth occurs for both melittin<sup>PA2</sup> and melittin<sup>pure</sup>, however, it is all noticeably slower and smaller for melittin<sup>pure</sup> at 25°C. At 37°C the kinetics are comparable for both melittin<sup>PA2</sup> and melittin<sup>pure</sup>, though melittin<sup>PA2</sup> achieves a higher magnitude *LD* signal. There is no evidence of micellisation on an hours to days timescale at either 25°C or 37°C with melittin<sup>pure</sup>. When we added PA2 (at the upper bound of that present in melittin<sup>PA2</sup> from Sigma) to melittin<sup>pure</sup>, then the rates/intensities observed with melittin<sup>PA2</sup> were recovered (or indeed exceeded).

We also investigated the effect of PA2 on DMPC liposomes. The DLS data of Figure c show that PA2 alone does disrupt the liposomes at 25°C, however, the time takes about twenty times longer than that of the combined melittin/PA2 preparation. There was no PA2 *LD* or *CD* evident in this sample due to the low protein concentration of PA2.

3/3/10 0:08

**Comment:** Where is this data?  
Correct y-axis scale and remove white grid lines



3/3/10 0:08

**Comment:** Where is this data?

Correct y-axis scale and remove white grid lines

Figure (a) LD and (b) DLS of melittin<sup>pure</sup> (0.1 mg/mL) in DMPC (at molar ratio of lipid: peptide of 100:1) at (i) 25°C and (ii) 37°C. (c) DLS of DMPC liposomes with PA2 (0.05 Units) at different temperatures.

To determine how the PA2-catalysed DMPC hydrolysis affected melittin interaction with DMPC liposomes we adapted a TLC method taken from the Avanti web site and developed a MALDI methodology to follow any changes in the lipids during the insertion reaction. We first established that both the TLC plate and the MALDI matrix (DHB) quenched the enzyme-catalyzed hydrolysis of DMPC, so it was a straightforward matter to sample a reaction at different time-points and measure the lipid content. As shown in Figure the intensity of the DMPC signal reduces and that of lysoPC grows at compensating rates. The TLC results confirm the MALDI data (data not shown). At about  $t=6$  minutes (where the intensities of the DMPC and lysoPC peaks are comparable) the liposomes fragment into smaller particles. Not surprisingly, the  $LD$  signal is maximum just before this time point.

EDTA is known to suppress the activity of PA2.<sup>21</sup> Addition of EDTA (2 mM) to the DMPC/melittin<sup>PA2</sup> reaction mixture slowed down the whole process (insertion and membrane disruption) to a timescale of tens of hours.

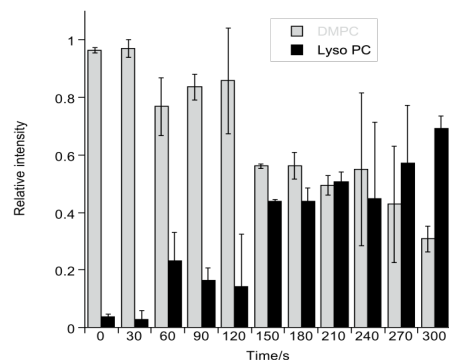


**Figure** MALDI analysis of the lipids present after melittin<sup>PA2</sup> was added to DMPC liposomes. Experimental details are as for Figure . Timepoints are indicated on the figure.

There is evidence in the literature that PA2 activity increases when there are more defects in the membrane,<sup>ref???</sup> John *i.e.* close to the transition temperatures and/or induced by melittin binding, especially in the gel phase).<sup>38</sup> This would make the activities of PA2 and melittin synergistic. The activity of PA2 is generally low??? on saturated membranes on either side of the transition temperature. It is somewhat counter-intuitive that the insertion is faster in the more rigid lower temperature environment, but this may be the underlying reason.

### Melittin insertion as a function of lipid composition

Biological membranes are made predominately of *sn*-1 saturated, *sn*-2 unsaturated acyl chains or even of phospholipids with two polyunsaturated acyl chains. Phospholipids with polyunsaturated acyl chains are known to influence membrane dynamics.<sup>39, 40</sup> Further, it has been shown that the degree of unsaturation of a membrane modulates the membrane-disruption action of melittin (lytic power and bilayer micellisation).<sup>36</sup> This has been claimed to be at least in part due to the secondary structure of melittin changing with the membrane. However, as discussed above, their observed increase in the 222 nm CD band is more likely to be due to better packing of the hydrophobic phase. We therefore chose to consider the effect of melittin<sup>PA2</sup> on a range of lipids formed into liposomes.

DLS showed us a first difference between the lipids, namely that the vesicles made from unsaturated lipids by extruding through a 100 nm polycarbonated membrane were approximately twice the size of those made from saturated vesicles (which were ~110 nm). This reflects the greater flexibility of the unsaturated lipid vesicles operating during the extrusion process.

The maximum LD signals, obtained after the time indicated in the figure, are shown in Figure . From the data it can be concluded that the orientation of melittin is similar in all the systems studied. Although the unsaturated lipids have slightly larger signals, as their lipids are of higher molecular weight and the sample viscosity is somewhat higher we cannot ascribe any significance to this. Another key parameter is how quickly that maximum signal is obtained. The peptide adopts its maximum LD signal in the order indicated in Table . Somewhat surprisingly the slightly higher temperature but still less flexible saturated gel-phase membranes obtain maximum transmembrane orientation (LD maximum) more quickly than the unsaturated more flexible ones. Addition of negative lipids speeds the process up for the saturated lipids whereas it slows it down further for the unsaturated one. Pure DPPC (Table 2, Figure ) shows no insertion. Overall, the LD data suggest that flexibility of the membrane slows down the insertion process but the end product is better oriented.

Not only does the membrane provide an environment for the peptide, it is also affected by the peptide as summarized in Table . Two competing perturbations to the membranes occur: fusion and micellisation. Negative charge and unsaturation increase the tendency for the liposomes to grow (presumably by fusion) in size whereas saturation (or more rigid membranes, *e.g.* the gel phase of DMPC) favours membrane micellisation. However, this conclusion is over simplistic since POPC with one double bond is dominated by micellisation.



**Table Summary of kinetic data for melittin as a function of lipid properties. Ranking is as follows: 0 denotes none; 1 denotes least flexible/rate of insertion/micellisation/fusion; 2 denotes slightly more *etc.***

|                                  | DOPC      | POPC/DPPG      | POPC      | DMPC        | DPPG | DMPC         | DPPC/DPPG | DPPC      |
|----------------------------------|-----------|----------------|-----------|-------------|------|--------------|-----------|-----------|
|                                  | 18:1_18:1 | 18:1_16:0/16:0 | 18:1_16:0 | 37°<br>14:0 | 16:0 | 25°C<br>14:0 | 16:0/16:0 | 16:0      |
| Estimate of membrane flexibility | 8         | 7              | 5         | 5           | 1    | 2            | 2         | 2         |
| Negative charge                  | 0         | 1              | 0         | 0           | 2    | 0            | 1         | 0         |
| LD intensity                     | 7         | 3              | 2         | 4           | 5    | 6            | 1         | 0         |
| Rate of insertion                | 1         | 2              | 3         | 4           | 5    | 6            | 7         | 0 (no LD) |
| Micellisation                    | 0         | 0              | 1         |             | 0    | 3            | 2         | 4         |
| Fusion                           | 3         | 4              | 2         |             | 0    | 1            | 0         | 5         |

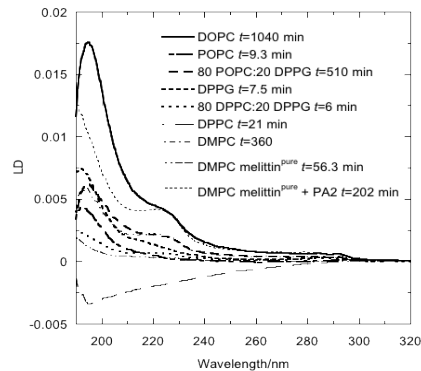


**Figure Maximum LD spectra obtained for melittin<sup>PA2</sup> (0.1 mg/mL) added to liposomes at lipid:peptide ratio of 100:1. Times and lipids are indicated on the figure.**

### Conclusion

For the first time, in this work, flow aligned linear dichroism has been applied to study the orientation of melittin in the membrane-mimicking environment of a liposome. It is the ideal technique for such real-time measurements. Overall, the pattern is a very complicated molecular process even for a simple peptide such as melittin, however, LD helps one clearly identify when insertion is happening which improves our ability to analyse peptide/membrane interactions. However, LD does not stand on its own and needs to be complemented by a range of other biophysical techniques.

Melittin is co-purified from bee venom with phospholipase A2. They were known to affect each other’s behaviour. We developed TLC and MALDI methods from those available in the literature to follow the lipid kinetics in parallel with the LD experiments. We found that PA2

speeded up the insertion of melittin (as measured by the increase of the LD signal) and also speeded up any membrane disruption that melittin induces. Similarly, melittin speeds up the phospholipase action of PA2. However, by comparing melittin co-purified with phospholipase A2, pure melittin and pure melittin doped with phospholipase A2 we concluded there was no other difference in behaviour. We therefore focused our analysis on melittin with catalytic amounts of the enzyme as a more representative sample of the action of native melittin.

For the first time we have surveyed the behaviour of melittin with a range of lipids. Overall our conclusions about melittin are that melittin is helical with all the lipids studied, though random coil in aqueous solution. When added to liposomes it rapidly folds and then inserts more or less parallel to the membrane normal. The membrane insertion behaviour of melittin varies with lipid and membrane phase. In general terms, the insertion is faster with more rigid lipids but generally reaches a higher level (as indicated by LD magnitude) with less rigid lipids. Inclusion of 20% negatively-charged lipids affects the insertion, speeding the process up for the saturated lipids but slowing it down further for the unsaturated one. We detected no insertion with the liposomes made from 100% of the long chain saturated lipid DPPC. Any assessment of insertion effectiveness is affected by how the melittin is perturbing the membrane: it can induce both fusion and micellisation—the latter leading to no LD while retaining insertion into the membrane. Saturated lipids are more prone to micellisation.

The mechanistic conclusions to be deduced from this work relate to the insertion/fusion/micellation properties of melittin with a range of lipids, which suggest a mechanism whereby melittin in collaboration with phospholipaseA2 acts on membranes to insert and then degrade the lipids to facilitate micellisation. This will enable the melittin to be recycled to affect more membranes than the initial target. These observations are consistent with the recent realization that the way many cationic amphiphilic drugs work is by catalysing the chemical degradation of the phospholipid fabric of plasma membranes. Melittin as with other peptides thus does not simply interact passively with cellular membranes as postulated by current drug translocation mechanisms, rather it is an active physical and chemical process.<sup>20, 41, 42</sup>

## References

1. Wallin, E.; von Heijne, G., *Protein Science* **1998**, 7, 1029-1038.
2. Terstappen, G. C.; Reggiani, A., *Trends Pharmacol Sci* **2001**, 22, 23-26.
3. Vaara, M., New approaches in peptide antibiotics. *Curr. Opin. Pharmacology* **2009**, 9, 571-576.
4. Hancock, R. E. W.; Chappel, D. S., Antimicrobial agents and chemotherapy. *Peptide Antibiotics* **1999**, 43, (6), 1317-1323.

5. Ardhammar, M.; Mikati, N.; Nordén, B., Chromophore orientation in liposome membranes probed with flow linear dichroism. *J. Amer. Chem. Soc.* **1998**, 120, 9957-9958.
6. Rajendra, J.; Baxendale, M.; Dit Rap, L. G.; Rodger, A., Flow linear dichroism to probe binding of aromatic molecules and DNA to single walled carbon nanotubes. *J. Amer. Chem. Soc.* **2004**, 126, 11182-11188.
7. Rajendra, J.; Damianoglou, A.; Hicks, M.; Booth, P.; Rodger, P. M.; Rodger, A., Quantitation of protein orientation in flow-oriented unilamellar liposomes by linear dichroism. *Chemical Physics* **2006**, 326, (1), 210-220.
8. Esbjorner, E. K.; Caesar, C. E. B.; Albinsson, B.; Lincoln, P.; Nordén, B., Tryptophan orientation in model lipid membranes. *Biochem. Biophys. Res. Comm.* **2007**, 361, 645-650.
9. Esbjörner, E. K.; Oglcka, K.; Lincoln, P.; Gräslund, A.; Nordén, B., Membrane binding of pH-sensitive influenza fusion peptides. Positioning, configuration, and induced leakage in a lipid vesicle model. *Biochemistry* **2007**, 46, 13490-13504.
10. Hicks, M. R.; Dafforn, T.; Damianoglou, A.; Wormell, P.; Rodger, A.; Hoffmann, S. V., Synchrotron radiation linear dichroism spectroscopy of the antibiotic peptide gramicidin in lipid membranes. *The Analyst* **2009**, 134(8), 1623-1628.
11. Hicks, M. R.; Damianoglou, A.; Rodger, A.; Dafforn, T. R., Folding and membrane insertion of the pore-forming peptide gramicidin occur as a concerted process. *Journal of molecular biology* **2008**, 383, (2), 358-66.
12. Ennaceur, S. M.; Hicks, M. R.; Pridmore, C. J.; Dafforn, T. R.; Rodger, A.; Sanderson, J. M., Peptide adsorption to lipid bilayers: slow rearrangement processes revealed by linear dichroism spectroscopy. *Biophys J* **2009**, 96, (4), 1399-1407.
13. Raghuraman, H.; Chattopadhyay, A., Melittin: a Membrane-active Peptide with Diverse Functions, *Biosci Rep.*, **2007**, 27, 189-223.
14. J. C. Talbot, Conformational change and self association of monomeric melittin. *FEBS Lett.* **1979**, 102, 191-193.
15. Dempsey, C. E., *Biochim. Biophys. Acta* **1990**, 1031, 143-161.
16. Shai, Y., Molecular recognition between membrane-spanning polypeptides. *TIBS* **1995**, 20, 460-464.
17. Papo, N.; Shai, Y., Exploring Peptide Membrane Interaction Using Surface Plasmon Resonance: Differentiation between Pore Formation versus Membrane Disruption by Lytic Peptides. *Biochemistry* **2003**, 42, 458-466.
18. Bogaart, G. v. d.; Guzmán, J. V.; Mika, J. T.; Poolman, B., On the Mechanism of Pore Formation by Melittin, *The Journal of biological chemistry.* **2008**, 283, 33854-33857.
19. Manna, M.; Mukhopadhyay, C., Cause and Effect of Melittin-Induced Pore Formation: A Computational Approach. *Langmuir* **2009**, 25, 12235-12242.
20. Casey, D. R.; Sebai, S. C.; Shearman, G. C.; Ces, O.; Law, R. V.; Gee, A. D.; Templer, R. H., Formulation Affects the Rate of Membrane Degradation Catalyzed by Cationic Amphiphilic Drugs. *Ind. Eng. Chem. Res.* **2008**, 47, 650-665.
21. Dempsey, C. E.; A., W. A., Deuterium and Phosphorus-31 Nuclear Magnetic Resonance Study of the Interaction of Melittin with DMPC bilayers and the effects of contaminating phospholipase A2. *Biochemistry* **1987**, 26, 5803-5811.
22. Rodger, A.; Rajendra, J.; Marrington, R.; Ardhammar, M.; Nordén, B.; Hirst, J. D.; Gilbert, A. T. B.; Dafforn, T. R.; Halsall, D. J.; Woolhead, C. A.; Robinson, C.; Pinheiro, T. J.; Kazlauskaitė, J.; Seymour, M.; Perez, N.; Hannon, M. J., Flow oriented linear dichroism to probe protein orientation in membrane environments. *Phys. Chem. Chem. Phys.* **2002**, 4, 4051-4057.
23. Rodger, A.; Patel, K. K.; Sanders, K. J.; Datt, M.; Sacht, C.; Hannon, M. J., Anti-tumour platinum acylthiourea complexes and their interactions with DNA. *Dalton* **2002**, 3656-3663.

24. Rodger, A.; Marrington, R.; Geeves, M. A.; Hicks, M.; de Alwis, L.; Halsall, D. J.; Dafforn, T. R., Looking at long molecules in solution: what happens when they are subjected to Couette flow? *Physical Chemistry Chemical Physics* **2006**, 8, (27), 3161-3171.
25. Marrington, R.; Dafforn, T. R.; Halsall, D. J.; Rodger, A., Micro volume Couette flow sample orientation for absorbance and fluorescence linear dichroism. *Biophys. J.* **2004**, 87, 2002-2012.
26. Marrington, R.; Dafforn, T. R.; Halsall, D. J.; Hicks, M.; Rodger, A., Validation of new microvolume Couette flow linear dichroism cells. *Analyst* **2005**, 130, 1608-1616.
27. Constantinescu, I.; Lafleur, M., Influence of the lipid composition on the kinetics of concerted insertion and folding of melittin in bilayers. *Biochim. Biophys. Acta* **2004**, 1667, 26-37.
28. Sui, S., Conformational Changes of Melittin upon Insertion into Phospholipid Monolayer and Vesicle. *J. Biochem.* **1994**, 116, 482-487.
29. Veen, M. V.; Georgiou, G. N.; Drake, A. F.; Cherry, R. J., Circular-dichroism and fluorescence studies on melittin: effects of C-terminal modifications on tetramer formation and binding to phospholipid vesicles. *Biochem. J.* **1995**, 305, 785-790.
30. Andersson, A.; Biverstahl, H.; Nordin, J.; Lindahl, E.; Mäler, L., The membrane induced structure of melittin is correlated with the fluidity of the lipids. *Biochim. Biophys. Acta* **2007**, 1768, 115-121.
31. Ghosh, A. K.; Rukmini, R.; Chattopadhyay, A., Modulation of Tryptophan Environment in Membrane-Bound Melittin by Negatively Charged Phospholipids: Implications in Membrane Organization and Function, . *Biochemistry* **1997**, 36, 14291-14305.
32. Raghuraman, H.; Chattopadhyay, A., Interactions of melittin with membrane cholesterol: A fluorescence approach, . *Biophys. J.* **2004**, 87, 2419-2432.
33. Ladokhin, A. S.; White, S. H., *J. Mol. Biol.* **1999**, 285, 1363-1369.
34. Lazarova, T.; Brewin, K. A.; Stoeber, K.; Robinson, C. R., *Biochemistry* **2004**, 43, 12945-12954.
35. Thevenin, D.; Lazarova, T.; Roberts, M. F.; Robinson, C. R., *Protein Science* **2005**, 14, 2177-2186.
36. Raghuraman, H.; Chattopadhyay, A., Influence of lipid chain unsaturation on membrane bound melittin : a fluorescence approach. *Biochim. Biophys. Acta* **2004**, 1665, 29-39.
37. Nordén, B.; Rodger, A.; Dafforn, T., *Linear dichroism and circular dichroism: A textbook on polarized-light spectroscopy* . Royal Society of Chemistry: Cambridge, 2010.
38. Bell, J. D.; Burnside, M.; Owen, J. A.; Royall, M. L.; Baker, M. L., Relationships between Bilayer Structure and Phospholipase A2 Activity: Interactions among Temperature, Diacylglycerol, Lysolecithin, Palmitic Acid, and Dipalmitoylphosphatidylcholine. *Biochemistry* **1996**, 35, 4945-4955.
39. Mitchell, D. C., Molecular Order and Dynamics in Bilayers Consisting of Highly Polyunsaturated Phospholipids. *Biophys. J.* **1998**, 74, 879-891.
40. Saiz, L., Computer Simulation Studies of Model Biological Membranes. *Acc. Chem. Res.* **2002**, 35, 482-489.
41. Baciú, M.; Sebai, S. C.; Ces, O.; Mulet, X.; Clarke, J. A.; Shearman, G. C.; Law, R. V.; Templer, R. H.; Plisson, C.; Parker, C. A.; Gee, A., *Philosophical Transactions of the Royal Society a-Mathematical Physical and Engineering Sciences*, **2006**, 364, 2597-2614.
42. Shearman, G. C.; Attard, G. S.; Hunt, A. N.; Jackowski, S.; Baciú, M.; Sebai, S. C.; Mulet, X.; Clarke, J. A.; Law, R. V.; Plisson, C.; Parker, C. A.; Gee, A.; Ces, O.; Templer, R. H., *Biochemical Society Transactions* **2007**, 35, 498-501.